

A SEMI-ANALYTICAL APPROACH FOR DYNAMIC STRESS CONCENTRATION FACTOR OF HELMHOLTZ PROBLEMS WITH CIRCULAR HOLES

Po-Yuan Chen, Chia-Tsung Chen and Jeng-Tzong Chen

Department of Harbor and River Engineering

National Taiwan Ocean University

Keelung 20224, Taiwan, R. O. C.

M93520010@mail.ntou.edu.tw

ABSTRACT

In this paper, a semi-analytical approach is developed for the problem of dynamic stress concentration around circular cavities due to shear waves. To fully capture the circular geometries, separate expressions of fundamental solutions in the polar coordinate and Fourier series for boundary densities are adopted. The main gain of using degenerate kernels is free of calculating the principal values. An adaptive observer system is addressed to fully employ the property of degenerate kernels in the polar coordinate. After moving the null-field point to the boundary and matching the boundary conditions, a linear algebraic system is obtained and the unknown coefficients in the algebraic system can be easily determined. The present method is seen as a “semi-analytical” solution since error only attributes to the truncation of Fourier series. The proposed formulation is generalized to a half-plane problem with a circular cavity.

Keywords: SH-wave, dynamic stress concentration, half-plane problem, circular cavity, null-field integral equation, degenerate kernel, Fourier series, Helmholtz equation.

1. INTRODUCTION

The concentration of stress around holes plays an important role in promoting the design criteria for higher factors of safety. Not only static but also dynamic stress concentration factors have been investigated in the literature. For a simple case, an analytical solution may be available. However, solutions for problems with several holes may resort to the numerical techniques. To develop a semi-analytical approach is not trivial. This is the main goal of this paper.

For the problems with circular boundaries, the Fourier series expansion method is specially suitable to obtain the analytical solution. For Laplace problems, Chou [1] used the complex variable boundary element method (CVBEM) to solve the

stress field around holes in antiplane shear. Thakur *et al.* [2] used a second-order accurate block-structured finite-volume method with periodic boundary conditions along the cylinder axis to solve the wake flow of single and multiple yawed cylinders. Wang [3] solved the unsteady problem of two parallel circular cylinders, moving in an inviscid fluid by exploring the technique of conformal mapping. For Helmholtz problems, Elsherbeni and Hamid [4] used the method of moments to solve the scattering problem by parallel conducting circular cylinders. They also divided the total scattered field into two components, namely a noninteraction term and the term due to all interactions between the cylinders. Chen *et al.* [5] employed the dual BEM to solve the exterior acoustic problems with circular boundaries. Grote and Kirsch [6] utilized Dirichlet to Neumann (DtN) method to solve multiple scattering problems of multiple cylinders. The DtN solution was obtained by combining contributions from multiple outgoing wave fields. Kawase [7] used the BEM in the domain of wave number, in which the discrete wave number Green's function was adopted to solve the scattering problem of a semi-cylindrical canyon subject to the plane waves. It compared well with the analytical solution which was derived by Trifunac [8]. For the biharmonic problems, Ling [9] used bipolar coordinates to solve a plate containing two circular holes. Howland and Knight [10] used the rectangular coordinate system to solve a plate containing groups of circular holes. According to the literature review, it is observed that exact solutions for boundary value problems are only limited for simple cases, *e.g.* a cylinder radiator and scatter, half-plane with a semi-circular canyon, a hole under half-plane and two holes in infinite plate. Therefore, proposing a systematic approach for solving BVP with circular boundaries of various numbers, positions and radii is our goal in this paper.

In this paper, the boundary integral equation method (BIEM) is utilized to solve the exterior radiation and scattering problems with circular boundaries. To fully utilize the geometry of circular boundary, not only Fourier series expansion for

boundary densities but also the degenerate kernel for fundamental solutions is incorporated into the null-field integral equation. Senses of principal values are not required to determent all the improper integrals, but using only series summation. In integrating each circular boundary for the null-field equation, the adaptive observer system of polar coordinate is considered to fully employ the property of degenerate kernel. For the hypersingular equation, vector decomposition for the radial and tangential gradients is carefully considered, especially in the eccentric case. Scattering problem subject to the incident wave is decomposed into two parts, incident plane wave field and radiation field. The radiation boundary condition is the minus quantity of incident wave function for matching the boundary condition of total wave. Three cases are used to check the validity of our formulation.

2. PROBLEM STATEMENT AND INTERGAL FORMULATION

2.1 Problem statement

The governing equation of the acoustic problem is the Helmholtz equation

$$(\nabla + k)^2 w(x) = 0, \quad x \in D, \quad (1)$$

where ∇^2 , k and D are the Laplacian operator, the wave number, and the domain of interest, respectively. Consider the radiation and scattering problems containing N randomly distributed circular holes centered at the position vector ζ_j ($j=1, 2, \dots, N$).

The displacement field of the SH-wave is defined as:

$$u = v = 0, \quad w = w(x, y), \quad (2)$$

where w is the only nonvanishing component of displacement with respect to the Cartesian coordinate which is a function of x and y . For a linear elastic body, the stress components are [11]

$$\sigma_{13} = \sigma_{31} = \mu \frac{\partial w}{\partial x}, \quad (3)$$

$$\sigma_{23} = \sigma_{32} = \mu \frac{\partial w}{\partial y}, \quad (4)$$

where μ is the shear modulus. The equilibrium equation can be simplified to

$$\frac{\partial \sigma_{31}}{\partial x} + \frac{\partial \sigma_{32}}{\partial y} = 0. \quad (5)$$

By substituting Eqs. (3) and (4) into (5), we have Eq. (1). What is taken into consideration is an infinite medium subject to N traction-free circular holes

bounded by the B_k contour and $k = 1, 2, \dots, N$. The medium is under SH wave equivalently under the displacement

$$w^i = W_0 e^{ik(x \sin \gamma + y \cos \gamma)}, \quad (6)$$

where W_0 is the constant amplitude. The total stress field in the medium is decomposed into

$$\sigma_{31} = \sigma_{31}^s + \sigma_{31}^i, \quad (7)$$

$$\sigma_{32} = \sigma_{32}^s + \sigma_{32}^i, \quad (8)$$

and the total displacement can be given as

$$w = w^s + w^i, \quad (9)$$

where the superscript “s” denotes the part needed to be solved after decomposition.

Therefore, the scattering problem is reduced to find the displacement w^s which satisfies the Helmholtz equation and the boundary conditions that will be elaborated on later. The problem can be converted into the solution of the Helmholtz problem for w^s :

$$(\nabla + k)^2 w^s(x) = 0, \quad x \in D. \quad (10)$$

The shear stress components, σ_{rz} and $\sigma_{\theta z}$, can be superimposed by using σ_{31} and σ_{32}

$$\sigma_{rz} = \mu \frac{\partial w}{\partial \mathbf{n}}, \quad (11)$$

$$\sigma_{\theta z} = \mu \frac{\partial w}{\partial \mathbf{t}}, \quad (12)$$

where \mathbf{n} and \mathbf{t} are the normal and tangent directions, respectively. Before determining σ_{rz} and $\sigma_{\theta z}$ on the interior point, we should calculate σ_{31}^s and σ_{32}^s by implementing the hypersingular equation in the real computation. For shear stress $\sigma_{\theta z}$ on the boundary, the same procedure of vector decomposition is required, and the nondimensional stress $\sigma_{\theta z}^*$ is defined as:

$$\sigma_{\theta z}^* = \left| \frac{\sigma_{\theta z}}{\sigma_0} \right|, \quad (13)$$

where $\sigma_0 = \mu k W_0$ is the maximum stress of incident wave.

2.2 Dual boundary integral formulation

In order to solve the solution of w^s , we propose a unified null-field integral equation. Based on the dual boundary integral formulation of the domain point, we have

$$2\pi w^s(x) = \int_B T(s, x) w^s(s) dB(s) - \int_B U(s, x) t^s(s) dB(s), \quad x \in D, \quad (14)$$

$$2\pi t^s(x) = \int_B M(s, x) w^s(s) dB(s) \quad (15)$$

$$- \int_B L(s, x) t^s(s) dB(s), x \in D,$$

where s and x are the source and field points, respectively, $t^s(s)$ is the directional derivative of $w^s(s)$ along the outer normal direction at s . The $U(s, x)$, $T(s, x)$, $L(s, x)$ and $M(s, x)$ are four kernel functions [12]

$$U(s, x) = \frac{-i\pi H_0^{(1)}(kr)}{2}, \quad (16)$$

$$T(s, x) = \frac{\partial U(s, x)}{\partial n_s} = \frac{-ik\pi H_1^{(1)}(kr)}{2} \frac{y_i n_i}{r}, \quad (17)$$

$$L(s, x) = \frac{\partial U(s, x)}{\partial n_x} = \frac{ik\pi H_1^{(1)}(kr)}{2} \frac{y_i \bar{n}_i}{r}, \quad (18)$$

$$M(s, x) = \frac{\partial^2 U(s, x)}{\partial n_x \partial n_s} \quad (19)$$

$$= \frac{-ik\pi}{2} \left[-k \frac{H_2^{(1)}(kr)}{r^2} y_i y_j n_i \bar{n}_j + \frac{H_1^{(1)}(kr)}{r} n_i \bar{n}_i \right],$$

where $H_n^{(1)}(kr)$ is the n -th order Hankel function of the first kind, $r = |x - s|$, $y_i = s_i - x_i$, $i^2 = -1$, n_i and \bar{n}_i are the i -th components of the outer normal vectors at s and x , respectively. Eqs. (14) and (15) are referred to the singular and hypersingular boundary integral equations (BIE), respectively.

2.3 Null-field integral formulation in conjunction with the degenerate kernel and Fourier series

By collocating x outside the domain ($x \in D^c$), we obtain the null-field integral equations as shown below:

$$0 = \int_B T(s, x) w^s(s) dB(s) \quad (20)$$

$$- \int_B U(s, x) t^s(s) dB(s), x \in D^c,$$

$$0 = \int_B M(s, x) w^s(s) dB(s) \quad (21)$$

$$- \int_B L(s, x) t^s(s) dB(s), x \in D^c,$$

where the collocation point x locates on the outside of the domain and can be on the boundary in real computations. By using the polar coordinate, we can express $x = (\rho, \phi)$ and $s = (R, \theta)$. The four kernels, U , T , L and M can be expressed in terms of degenerate kernels as shown below:

$$U(s, x) = \begin{cases} U^I(s, x) = \frac{-\pi i}{2} \sum_{m=-\infty}^{\infty} J_m(k\rho) H_m^{(1)}(kR) \cos(m(\theta - \phi)), R \geq \rho \\ U^E(s, x) = \frac{-\pi i}{2} \sum_{m=-\infty}^{\infty} H_m^{(1)}(k\rho) J_m(kR) \cos(m(\theta - \phi)), \rho > R, \end{cases}, \quad (22)$$

$$T(s, x) = \begin{cases} T^I(s, x) = \frac{-\pi k i}{2} \sum_{m=-\infty}^{\infty} J'_m(k\rho) H_m^{(1)}(kR) \cos(m(\theta - \phi)), R > \rho \\ T^E(s, x) = \frac{-\pi k i}{2} \sum_{m=-\infty}^{\infty} H_m^{(1)}(k\rho) J'_m(kR) \cos(m(\theta - \phi)), \rho > R, \end{cases} \quad (23)$$

$$L(s, x) = \begin{cases} L^I(s, x) = \frac{-\pi k i}{2} \sum_{m=-\infty}^{\infty} J'_m(k\rho) H_m^{(1)}(kR) \cos(m(\theta - \phi)), R > \rho \\ L^E(s, x) = \frac{-\pi k i}{2} \sum_{m=-\infty}^{\infty} H_m^{(1)}(k\rho) J'_m(kR) \cos(m(\theta - \phi)), \rho > R, \end{cases} \quad (24)$$

$$M(s, x) = \begin{cases} M^I(s, x) = \frac{-\pi k^2 i}{2} \sum_{m=-\infty}^{\infty} J'_m(k\rho) H_m^{(1)}(kR) \cos(m(\theta - \phi)), R \geq \rho \\ M^E(s, x) = \frac{-\pi k^2 i}{2} \sum_{m=-\infty}^{\infty} H_m^{(1)}(k\rho) J'_m(kR) \cos(m(\theta - \phi)), \rho > R, \end{cases} \quad (25)$$

where the superscripts I and E denote interior and exterior cases for the expressions of kernel. It is noted that the degenerate kernels for T and L expression for $\rho = R$ are not given since they are not continuous across the boundary. In order to incorporate with the Fourier series, the four kernel functions can be rewritten as [13]:

$$U(s, x) = \begin{cases} U^I(s, x) = \frac{-\pi i}{2} \sum_{m=0}^{\infty} \varepsilon_m J_m(k\rho) H_m^{(1)}(kR) \cos(m(\theta - \phi)), R \geq \rho \\ U^E(s, x) = \frac{-\pi i}{2} \sum_{m=0}^{\infty} \varepsilon_m H_m^{(1)}(k\rho) J_m(kR) \cos(m(\theta - \phi)), \rho > R, \end{cases}, \quad (26)$$

$$T(s, x) = \begin{cases} T^I(s, x) = \frac{-\pi k i}{2} \sum_{m=0}^{\infty} \varepsilon_m J'_m(k\rho) H_m^{(1)}(kR) \cos(m(\theta - \phi)), R > \rho \\ T^E(s, x) = \frac{-\pi k i}{2} \sum_{m=0}^{\infty} \varepsilon_m H_m^{(1)}(k\rho) J'_m(kR) \cos(m(\theta - \phi)), \rho > R, \end{cases}, \quad (27)$$

$$L(s, x) = \begin{cases} L^I(s, x) = \frac{-\pi k i}{2} \sum_{m=0}^{\infty} \varepsilon_m J'_m(k\rho) H_m^{(1)}(kR) \cos(m(\theta - \phi)), R > \rho \\ L^E(s, x) = \frac{-\pi k i}{2} \sum_{m=0}^{\infty} \varepsilon_m H_m^{(1)}(k\rho) J'_m(kR) \cos(m(\theta - \phi)), \rho > R, \end{cases}, \quad (28)$$

$$M(s, x) = \begin{cases} M^I(s, x) = \frac{-\pi k^2 i}{2} \sum_{m=0}^{\infty} \varepsilon_m J'_m(k\rho) H_m^{(1)}(kR) \cos(m(\theta - \phi)), R \geq \rho \\ M^E(s, x) = \frac{-\pi k^2 i}{2} \sum_{m=0}^{\infty} \varepsilon_m H_m^{(1)}(k\rho) J'_m(kR) \cos(m(\theta - \phi)), \rho > R, \end{cases}, \quad (29)$$

where ε_m is the Neumann factor

$$\varepsilon_m = \begin{cases} 1, & m = 0 \\ 2, & m = 1, 2, \dots, \infty \end{cases}. \quad (30)$$

In order to fully utilize the geometry of circular boundary, the potential w^s and its normal flux t^s can be approximated by employing the Fourier series. Therefore, we obtain

$$w^s(s) = a_0 + \sum_{n=1}^{\infty} (a_n \cos n\theta + b_n \sin n\theta), s \in B, \quad (31)$$

$$t^s(s) = p_0 + \sum_{n=1}^{\infty} (p_n \cos n\theta + q_n \sin n\theta), s \in B, \quad (32)$$

where a_0, a_n, b_n, p_0, p_n and q_n are the Fourier coefficients and θ is the polar angle which is equally discretized. Eqs. (20) and (21) can be easily calculated by employing the orthogonal property of Fourier series. In the real computation, only the finite M terms are used in the summation of Eqs. (31) and (32).

2.4 Adaptive observer system

Since the boundary integral equations are frame indifferent, *i.e.* rule of objectivity is obeyed. Adaptive observer system is chosen to fully employ the property of degenerate kernels. Figure 1 shows the boundary integration for the circular boundaries. It is worthy noted that the origin of the observer system can be adaptively located on the center of the corresponding circle under integration to fully utilize the geometry of circular boundary. The dummy variable in the integration on the circular boundary is just the angle (θ) instead of the radial coordinate (R). By using the adaptive system, all the boundary integrals can be determined analytically sense of principal value.

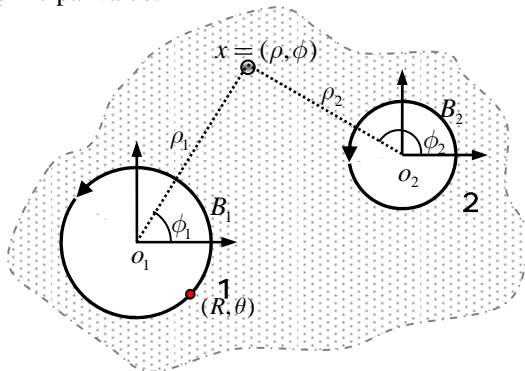


Figure 1. Adaptive observer system

2.5 Vector decomposition technique for the potential gradient in the hypersingular formulation

Since the hypersingular equation is a key ingredient to deal with fictitious frequency, potential gradient on the boundary is required to calculate. For the eccentric case, the field point and source point may not locate on the circular boundaries with the same center except the two points on the same circular boundary or on the annular cases. Special treatment for the normal and tangential derivatives should be taken care. As shown in Figure 2 where the origins of observer system are different, the true normal direction \hat{e}_1 with respect to the collocation point x on the B_j boundary should be superimposed by using the radial direction \hat{e}_3 and angular direction \hat{e}_4 .

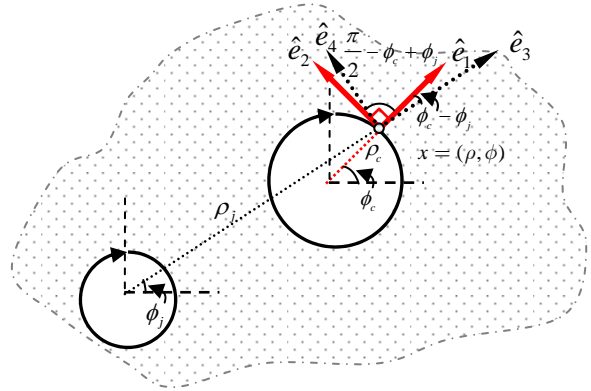


Figure 2. Vector decomposition for potential gradients in the hypersingular equation.

We call this treatment “vector decomposition technique”. According to the concept, Eqs. (24) and (25) can be modified as

$$L(s, x) = \begin{cases} \hat{L}^-(s, x) = \frac{-\pi k i}{2} \sum_{m=-\infty}^{\infty} J'_m(k\rho) H_m^{(1)}(kR) \cos(m(\theta - \phi)) \cos(\phi_c - \phi_j) \\ \quad - \frac{m}{k\rho} J_m(k\rho) H_m^{(1)}(kR) \sin(m(\theta - \phi)) \sin(\phi_c - \phi_j), R > \rho \\ \hat{L}^+(s, x) = \frac{-\pi k i}{2} \sum_{m=-\infty}^{\infty} H_m^{(1)}(k\rho) J'_m(kR) \cos(m(\theta - \phi)) \cos(\phi_c - \phi_j) \\ \quad - \frac{m}{k\rho} J_m(k\rho) H_m^{(1)}(kR) \sin(m(\theta - \phi)) \sin(\phi_c - \phi_j), \rho > R \end{cases}, \quad (33)$$

$$M(s, x) = \begin{cases} \hat{M}^-(s, x) = \frac{-\pi k i}{2} \sum_{m=-\infty}^{\infty} J'_m(k\rho) H_m^{(1)}(kR) \cos(m(\theta - \phi)) \cos(\phi_c - \phi_j) \\ \quad - \frac{m}{k\rho} J_m(k\rho) H_m^{(1)}(kR) \sin(m(\theta - \phi)) \sin(\phi_c - \phi_j), R \geq \rho \\ \hat{M}^+(s, x) = \frac{-\pi k i}{2} \sum_{m=-\infty}^{\infty} H_m^{(1)}(k\rho) J'_m(kR) \cos(m(\theta - \phi)) \cos(\phi_c - \phi_j) \\ \quad - \frac{m}{k\rho} J_m(k\rho) H_m^{(1)}(kR) \sin(m(\theta - \phi)) \sin(\phi_c - \phi_j), \rho > R \end{cases}, \quad (34)$$

2.6 Linear Algebraic Equation

In order to calculate the $2M+1$ unknown Fourier coefficients, $2M+1$ boundary points on each circular boundary are needed to be collocated. By moving the null-field point on the k th circular boundary for Eqs. (20) And (21), we have

$$0 = \sum_{j=1}^{N_c} \int_{B_j} T(s, x_k) w^s(s) dB(s) - \sum_{j=1}^{N_c} \int_{B_j} U(s, x_k) t^s(s) dB(s), x_k \in D^f, \quad (35)$$

$$0 = \sum_{j=1}^{N_c} \int_{B_j} M(s, x_k) w^s(s) dB(s) - \sum_{j=1}^{N_c} \int_{B_j} L(s, x_k) t^s(s) dB(s), x_k \in D^c, \quad (36)$$

where N_c is the number of circles. It is noted that the path is anticlockwise for the outer circle. Otherwise, it is clockwise. For the B_j integral of the circular boundary, the kernels of $U(s, x)$, $T(s, x)$, $L(s, x)$ and $M(s, x)$ are respectively expressed in terms of degenerate kernels of Eqs. (22), (23), (33) and (34) with respect to the observer origin at the center of B_j . The boundary densities of $w^s(s)$ and $t^s(s)$ are substituted by using the Fourier series of Eqs. (31) and (32), respectively. In the B_j integration, we set the origin of the observer system to collocate at the center c_j of B_j to fully utilize the degenerate kernel and Fourier series. By moving the null-field point to the boundary B_k from outside of the domain, a linear algebraic system is obtained

$$[U]\{t^s\} = [T]\{w^s\}, \quad (37)$$

$$[L]\{t^s\} = [M]\{w^s\}, \quad (38)$$

where $[U]$, $[T]$, $[L]$ and $[M]$ are the influence matrices with a dimension of $N_c \times (2M+1)$ by $N_c \times (2M+1)$ and $\{t^s\}$ and $\{w^s\}$ denote the vectors for $t^s(s)$ and $w^s(s)$ of the Fourier coefficients with a dimension of $N_c \times (2M+1)$ by 1. where, $[U]$, $[T]$, $[L]$, $[M]$, $\{w^s\}$ and $\{t^s\}$ are defined as follows:

$$[U] = [U_{\alpha\beta}] = \begin{bmatrix} U_{00} & U_{01} & \cdots & U_{0N} \\ U_{10} & U_{11} & \cdots & U_{1N} \\ \vdots & \vdots & \ddots & \vdots \\ U_{N0} & U_{N0} & \cdots & U_{NN} \end{bmatrix}, \quad (39)$$

$$[T] = [T_{\alpha\beta}] = \begin{bmatrix} T_{00} & T_{01} & \cdots & T_{0N} \\ T_{10} & T_{11} & \cdots & T_{1N} \\ \vdots & \vdots & \ddots & \vdots \\ T_{N0} & T_{N0} & \cdots & T_{NN} \end{bmatrix}, \quad (40)$$

$$[L] = [L_{\alpha\beta}] = \begin{bmatrix} L_{00} & L_{01} & \cdots & L_{0N} \\ L_{10} & L_{11} & \cdots & L_{1N} \\ \vdots & \vdots & \ddots & \vdots \\ L_{N0} & L_{N0} & \cdots & L_{NN} \end{bmatrix}, \quad (41)$$

$$[M] = [M_{\alpha\beta}] = \begin{bmatrix} M_{00} & M_{01} & \cdots & M_{0N} \\ M_{10} & M_{11} & \cdots & M_{1N} \\ \vdots & \vdots & \ddots & \vdots \\ M_{N0} & M_{N0} & \cdots & M_{NN} \end{bmatrix}, \quad (42)$$

$$\{w^s\} = \begin{bmatrix} w_0^s \\ w_1^s \\ w_2^s \\ \vdots \\ w_N^s \end{bmatrix}, \quad \{t^s\} = \begin{bmatrix} t_0^s \\ t_1^s \\ t_2^s \\ \vdots \\ t_N^s \end{bmatrix}, \quad (43)$$

where the vectors $\{w_k^s\}$ and $\{t_k^s\}$ are in the form of $\{a_0^k \ a_1^k \ b_1^k \ \cdots \ a_M^k \ b_M^k\}^T$ and $\{p_0^k \ p_1^k \ q_1^k \ \cdots \ p_M^k \ q_M^k\}^T$; the first subscript “ α ” ($\alpha=0,1,2,\dots,N$) in the $[U_{\alpha\beta}]$ denotes the index of the α th circle where the collocation point is located and the second subscript “ β ” ($\beta=0,1,2,\dots,N$) denotes the index of the β th circle where the boundary data $\{w_k^s\}$ or $\{t_k^s\}$ are specified. The integral N is the number of circular holes in the domain and M indicates the highest harmonic of truncated terms in Fourier series. The coefficient matrix of the linear algebraic system is partitioned into blocks, and each diagonal block (U_{pp} , p no sum) corresponds to the influence matrices due to the same circle of collocation and Fourier expansion.

3. THE TECHNIQUE FOR SOLVING SCATTERING PROBLEMS IN THE HALF PLANE PROBLEMS

3.1 Decomposition of scattering problem into incident wave field and radiation problem

For the scattering problem subject to the incident wave, this problem can be decomposed into two parts. For matching the boundary condition, the radiation boundary condition is obtained as the minus quantity of incident wave function, e.g. $t^s = -t^i$ for the hard scatter or $w^s = -w^i$ for the soft scatter, respectively where the subscript s and i mean radiation and incidence, respectively. The radiation part can be solved by employing our method.

3.2 Image concept for solving the half-plane problem

For the half-plane problem with a circular cavity as shown in Figure 3 (a), we extend it to a full

plane with the scatter by using image concept such that our formulation can be applied. By introducing the symmetry condition ($t=0$) on the ground surface, we merge the half-plane domain into the full-plane problem in conjunction with the reflective wave as shown in Figure 3 (b). Figure 3 (c) shows the transformed problem in the full plane. To solve the problem, the decomposition technique is employed by introducing two plane waves, one is incident and the other is reflective, instead of only one incident wave. After taking the free body of Figure 3 (c) through the ground surface, we obtain the solution which satisfies the Helmholtz equation of Eq. (1) and all the boundary condition.

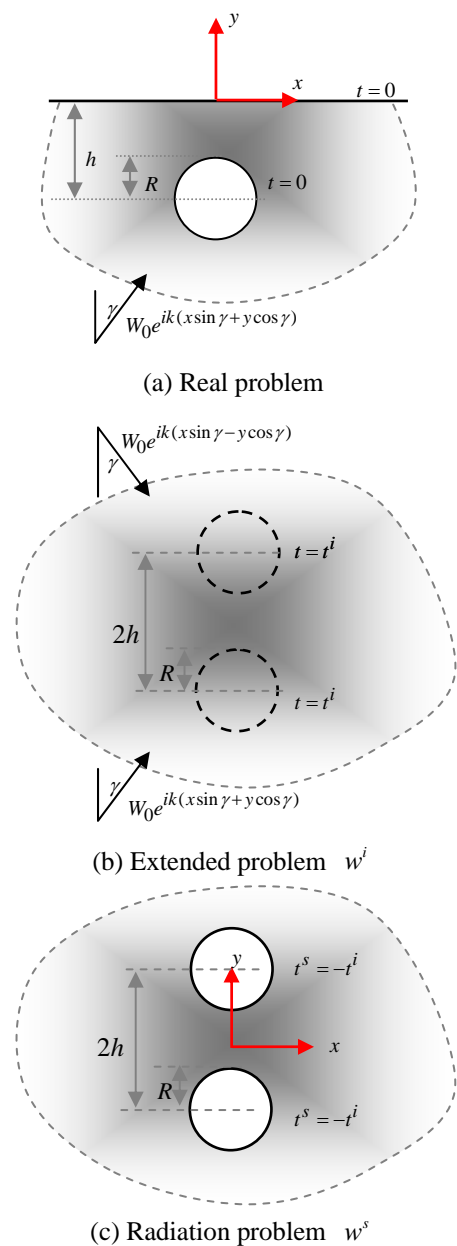


Figure 3 The image concept to transform half-plane problem to full plane problem

4. ILLUSTRATIVE EXAMPLES AND DISCUSSIONS

In order to check the validity of the present formulation, three cases are tested. All the numerical results are given below by using ten terms of Fourier series ($M = 10$).

Case1: Two circular cavities lie on the y-axis
 Figure 4 shows the geometry of the two circles whose radii are $a_1 = 1$ and $a_2 = 2$. For the static case, the displacement field of the anti-plane deformation is defined as:

$$w^\infty = \frac{\tau y}{\mu} \quad (44)$$

In the dynamic case with traction free condition on the circular boundaries, we assume an incident SH-wave as:

$$w^i = \frac{\tau y}{\mu} e^{ikx} \quad (45)$$

When k approaches zero, the problem is reduced to a static case. Figure 5 (a) and 5 (b) show the graph of the stress $\sigma_{\theta z}$ around the smaller circle. Three different distances ($d = 2, 0.1, 0.01$) between the two circles are considered. Our numerical results are well compared with the data of Honein's data [14] when k approaches zero ($k = 0.001$).

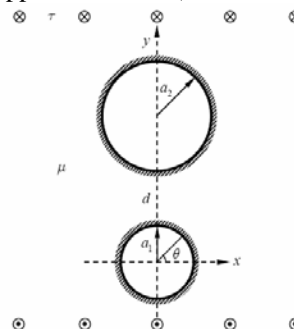


Figure 4

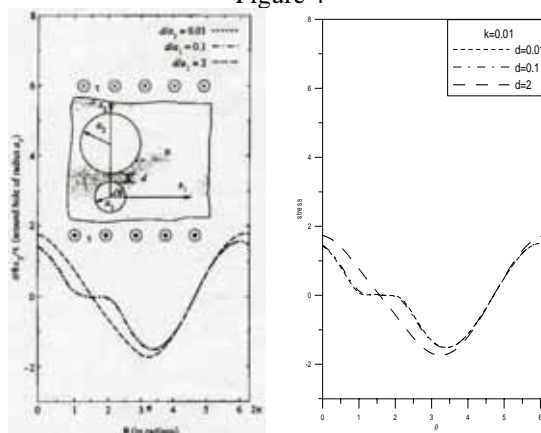


Figure 5 (a) Honein et al. [14] data

Figure 5 (b) $\sigma_{\theta z}$ around the smaller hole ($k = 0.001$)

Case2: A circular cylinder in an infinite space
 Consider a circular cylinder which is bounded by $r = a$ as shown in Figure 6. A shear wave is

defined by

$$u_x = 0, u_y = 0, u_z = W_0 e^{ikx}, \quad (46)$$

Figure 7 (a) and 7 (b) show the graph of the $\sigma_{\theta z}$ around the circular boundary. Traction free of the three lines are different cases with respect to $ka = 0.1, 1.0$ and 2.0 , respectively. It is worthy noted that our data agree well with the analytical solution of Pao and Mow's data [15] as shown below:

$$\sigma_{\theta z} = -\sigma_0 e^{-i(\omega t - \pi/2)} \sum_{n=0}^{\infty} \frac{\varepsilon_n i^{n-1}}{ka} \left[J_n'(ka) - \frac{J_n'(ka)}{H_n'(ka)} H_n^{(1)}(ka) \right] n \sin(n\theta) \quad (47)$$

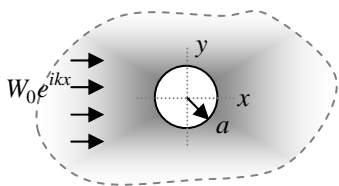


Figure 6

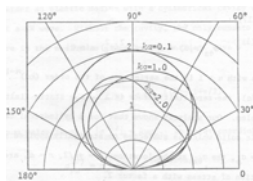


Figure 7 (a) DSCF (analytical solution)

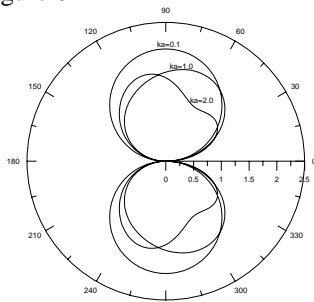


Figure 7 (b) the present method

Case3: A half-plane problem with a circular cavity
 Consider the scattering of SH-wave around a circular cavity in half plane as shown in Figure 8. The boundary conditions are traction free on the circular boundary and ground surface. Figures 9 and 10 are the Lin and Liu's data [16] which show the graph of the $\sigma_{\theta z}^*$ around the circular cavity. In the case of $\gamma = \pi/4, h/R = 1.5$, the maximum of $\sigma_{\theta z}^*$ is 3.75 on $\theta = 90^\circ$, while the maximum of $\sigma_{\theta z}^*$ is 2.16 on $\theta = 0^\circ$ and 180° for the case of $\gamma = \pi/4, h/R = 12$. Before solving the half-plane problem, an image method is employed to extend the domain to full domain with two holes by using symmetry condition as shown in Figure 3. Therefore, the developed program of our formulation can be easily applied to solve the problem. Our numerical results are compared with the data of Lin and Liu's data [16], good agreement is obtained.

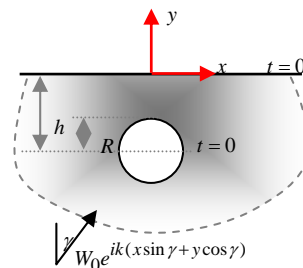


Figure 8 A cavity in the half plane subject to the incident SH wave

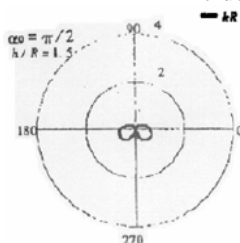


Figure 9 (a) Lin and Liu's result [16] ($\gamma = 0, h/R = 1.5, kR = 0.1$)

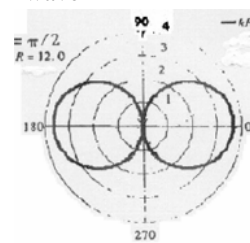


Figure 9 (b) Lin and Liu's result [16] ($\gamma = 0, h/R = 12, kR = 0.1$)

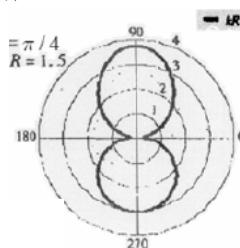


Figure 10 (c) Lin and Liu's result [16] ($\gamma = \pi/4, h/R = 1.5, kR = 0.1$)

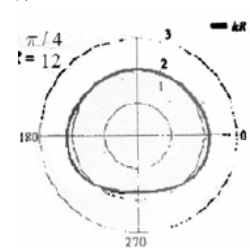


Figure 10 (d) Lin and Liu's result [16] ($\gamma = \pi/4, h/R = 12, kR = 0.1$)

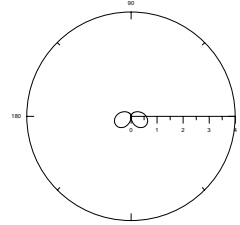


Figure 11 (e) ($\gamma = 0, h/R = 1.5, kR = 0.1$)

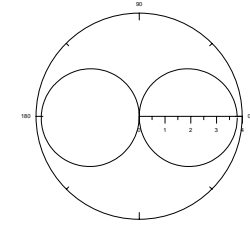


Figure 11 (f) ($\gamma = 0, h/R = 12, kR = 0.1$)

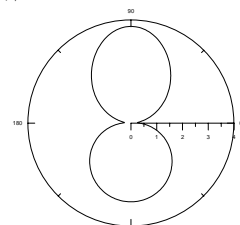


Figure 12 (g) ($\gamma = \pi/4, h/R = 1.5, kR = 0.1$)

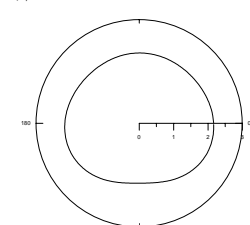


Figure 12 (h) ($\gamma = \pi/4, h/R = 12, kR = 0.1$)

5. CONCLUSIONS

For the radiation and scattering problems with circular boundaries, we have proposed a BIEM formulation by using degenerate kernels, null-field

integral equation and Fourier series in companion with adaptive observer systems and vector decomposition. This method is a semi-analytical approach for problems with circular boundaries since only truncation error in the Fourier series is involved. Also, the boundary dynamic stress and stress concentration factor are determined. The method shows great generality and versatility for the problems with multiple circular holes of arbitrary radii and positions. Half plane problem is a special case of the full plane by using the image concept.

REFERENCES

1. Chou S. I., "Stress field around holes in antiplane shear using complex variable boundary element method", *Transactions of the ASME*, Vol. 64 pp.432-435 (1997).
2. Thakur A. Liu X and Marshall J. S., "Wake flow of single and multiple yawed cylinders", *Transactions of the ASME*, Vol. 126, pp. 861-870 (2004).
3. Wang Q. X., "Interaction of two circular cylinders in inviscid fluid", *American Institute of Physics*, Vol. 16(12), pp. 4412-4425(2004).
4. Elsherbeni A. Z. and Hamid M., "Scattering by parallel conducting circular cylinders", *IEEE Trans. Antennas. Propag.* Vol. 35, pp. 355-358(1987).
5. Chen J. T., Chen C. T., Chen, K. H. and Chen, I. L., "On fictitious frequencies using dual BEM for non-uniform radiation problems of a cylinder", *Mech. Res. Comm.*, Vol. 27 (6), pp. 685-690 (2000).
6. Grote M. J. and Kirsch C., "Dirichlet to Neumann boundary conditions for multiple scattering problems", *J. Comp. Physics*, Vol. 201, pp. 630-650 (2004).
7. Kawase H., "Time-domain response of a semi-circular canyon for incident SV, P, and Rayleigh waves calculated by the discrete wavenumber boundary element method", *Bull. Seis. Soc. Am.*, Vol. 78, pp. 1415-1437 (1988).
8. Trifunac M. D. "Scattering of plane SH waves by a semi-cylindrical canyon", *Earthquake Eng. Struct. Dyn.*, Vol. 1, pp.267-281 (1973).
9. Ling C. B., "On the stress in a plate containing two circular holes", *J. App. Phys.*, Vol. 19, pp. 77-82 (1948).
10. Howland R. C. J. and Knight R. C., "Stress functions for a plate containing groups of circular holes", *Philos. Trans. R. Soc. Lond., Phys. Sci. Eng.*, Vol. 238, pp. 357-392 (1939).
11. Chen J. T., Shen W. C. and Wu A. C., "Null-field integral equations for stress field around circular holes under anti- plane shear", *Engineering Analysis with Boundary Elements*, accepted (2005).
12. Chen C. T., "Null-field integral equation approach for Helmholtz (interior and exterior

acoustic) problems with circular boundaries", Master Thesis, *Department of Harbor and River Engineering, National Taiwan Ocean University, Taiwan* (2005).

13. Chen C. T., Chen I. L. and Chen J. T., "Null-field integral equation approach for Helmholtz (interior and exterior acoustic) problems with circular boundaries", 電子計算機於土木水利工程應用研討會論文集, 台南 (2005).
14. Honein E., Honein T., Herrmann G., "On two circular inclusion in harmonic problems", *Quarterly of Applied Mathematics*, Vol. 50, pp.479-499 (1992).
15. Pao Y. H. and Mow C. C., *Diffraction of Elastic Waves and Dynamics Stress Concentrations*, New York (1971).
16. Lin H. and Liu D. K., "Scattering of SH-wave around a circular cavity in half space", *Earthquake Engineering and Engineering Vibration*, Vol. 22, No.2, pp.9-16 (2002).

半解析法求解含圓型孔洞赫姆茲問題之動應力集中因子

陳柏源、陳佳聰、陳正宗

國立台灣海洋大學河海工程學系

摘要

本文發展一新方法來求解由 SH 波引致於圓形孔洞周圍之動應力集中因子。為了充分利用圓形幾何外形，將基本解以分離核形式及邊界密度函數以傅立葉級數展開。使用退化核最主要可免去主值的計算。為了於極座標系統下充分使用退化核的特性，使用自適性參考座標系統。將觀察點移動至邊界並滿足邊界條件後，可獲得一個線性代數系統，且未知之傅立葉係數可輕易的被求得。誤差僅來自於所取之傅立葉級數項數的多寡。本法可廣泛應用於含圓形孔洞之全平面或半平面問題之分析。

關鍵字: 剪力波、動應力集中、半平面問題、圓孔洞、零場積分方程式，退化核、傅立葉級數、赫姆茲方程